

A steady state mathematical model for stepwise “slow-binding” reversible enzyme inhibition

Petr Kuzmič *

BioKin Ltd., 15 Main Street, Suite 232, Watertown, MA 02472, USA

Received 21 September 2007
Available online 17 January 2008

Abstract

The standard mathematical model for stepwise “slow-binding” enzyme inhibition ($E + I \rightleftharpoons EI \rightleftharpoons EI^*$) assumes that the initial enzyme–inhibitor complex EI is always at equilibrium with the free component species E and I . This assumption implies that the dissociation rate constant ($EI \rightarrow E + I$) is infinitely higher than the isomerization rate constant for $EI \rightarrow EI^*$. This paper presents a more general mathematical treatment, under the steady state approximation rather than the usual rapid-equilibrium approximation, whereby the two rate constants for the disappearance of EI are allowed to be comparable in magnitude. Experimentally relevant illustrative examples include discrimination between a single-step and a two-step mechanism for slow-binding inhibition kinetics.

© 2008 Published by Elsevier Inc.

Keywords: Enzyme kinetics; Inhibition; Slow-binding; Mathematics; Statistics; Regression; Modeling

“Slow-binding” reversible enzyme inhibitors are those that display a characteristic lag, or transient phase, in establishing their noncovalent bond to the target enzyme. Of course, slow binding is a relative concept. Virtually every enzyme inhibitor in existence can be forced to display a pre-steady state kinetic transient, either by shortening the observation time scale (e.g., in a stopped-flow instrument) or by drastically lowering all analytic concentrations, such that diffusion becomes rate limiting. This paper is concerned with those slow-binding inhibitors that show kinetic transients on the scale of seconds to minutes and even to hours, at total concentrations that are typical for standard *in vitro* enzyme assays (i.e., nanomolar to micromolar).

A necessary prerequisite for properly interpreting such transient kinetic data is having available a suitable mathematical model, that can be used for data fitting. Several useful mathematical models for slow-binding kinetics have been described in the literature (for review, see [1]). These existing mathematical models fall into two categories.

The first category of models, the most general and mathematically rigorous, consists of systems of simultaneous first-order ordinary differential equations (ODEs)¹. Such systems of differential equations are very easy to derive because they follow directly from the Law of Mass Action [1], but they are exquisitely difficult to solve. Solving a system of ODEs means calculating the concentration of reactants at any given time after the start of the reaction. In fact, the only way to solve a system of ODEs that typically arises in slow-binding inhibition kinetics is to use a highly specialized and numerically intensive computer algorithm.

The second category of existing mathematical models for slow-binding inhibition consists of simple algebraic formulas, that do not require intense iterative computations. These are closed-form kinetic equations of type $y = f(t, p)$, where t is reaction time, p are model parameters such as total concentration and rate constants, and y is the concentration of the given reactant. Such simple kinetic equations can be derived only by placing more or less severe restrictions or simplifying assumptions on the

* Fax: +1 617 209 1616.
E-mail address: pksci01@biokin.com.

¹ Abbreviation used: ODEs, ordinary differential equations.

hypothesized reaction mechanism. Relaxing one set of such restrictions, while still retaining the convenience of a simple algebraic formula as the final kinetic model, is the subject of this article.

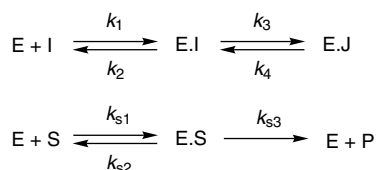
The reaction mechanism under investigation here is the stepwise binding. The enzyme E and the inhibitor I are assumed to form an initial complex, $E.I$, which subsequently rearranges to form the final complex $E.J$. The slow rearrangement, or isomerization, of the enzyme–inhibitor complex ($E.I \rightleftharpoons E.J$) is assumed to be the essence of the slow-binding kinetic transient. Cha [2] derived a kinetic equation for the appearance of the reaction product under the assumption that the inhibitor is only weakly bound to the enzyme (no inhibitor depletion). Later, Williams and Morrison [3] derived a more general kinetic equation, that does take inhibitor depletion (“tight binding”) into account.

Both Cha’s rate equation [2] and the more general rate equation proposed by Williams and Morrison [3] were derived under a crucially important simplifying assumption: both existing rate equations assume that the association and dissociation of the initially formed enzyme–inhibitor complex ($E + I \rightleftharpoons E.I$) is very much faster than either the forward or the reverse isomerization steps ($E.I \rightleftharpoons E.J$). This rapid-equilibrium approximation places a severe limit on the applicability of the kinetic equations for slow-binding that are currently in use.

This report describes an algebraic formula (a closed-form integrated rate equation) that does not imply any restrictions on the relative magnitude of rate constants appearing in the stepwise enzyme–inhibitor binding mechanism. This adds another tool to the currently available toolkit of mathematical models for slow-binding inhibition [2,3]. The potential use of the newly derived mathematical model is illustrated on several practically relevant examples.

Theory

Let us consider the stepwise enzyme–inhibitor binding mechanism shown in Scheme 1. The inhibitor I is assumed to compete with the substrate S for binding to the free enzyme E . We further assume that the inhibitor is bound only weakly (no tight binding [3]), such that the total or analytic concentration $[I]_0$ is always equal to the free inhibitor concentration $[I]$. We make the same assumption about substrate concentrations (negligibly small substrate depletion throughout the experiment; $[S]_0 = [S]$). Crucially



Scheme 1.

important, we do not assume that the inhibitor binding and dissociation steps are at rapid equilibrium. Relaxing the rapid-equilibrium requirement is the principal difference between the theoretical treatment presented in this paper and the other previously published reports on slow-binding inhibitor kinetics (for review, see [1]).

Under the assumptions described above, changes in the product concentration $[P]$ over time are described by a sum of two exponential terms plus one linear term, as shown in Eq. (1). The concentrations of enzyme–substrate complexes $E.I$ and $E.J$ evolve according to Eqs. (2), and (3), respectively. Various auxiliary expressions (v_0 , k , α , etc.) are defined in Eq. (4) through (15). The derivation of Eqs. (1) through (3)—the main theoretical result presented in this report—was performed by using the method of Laplace transforms [4]; the details are shown in the Appendix.

$$[P] = v_0 \gamma \left(1 + \frac{\beta - \alpha}{2\alpha} e^{-(k-\alpha)t} - \frac{\beta + \alpha}{2\alpha} e^{-(k+\alpha)t} \right) + v_s t. \quad (1)$$

$$[E.I] = [E.I]_\infty \left(1 + \frac{\delta - \alpha}{2\alpha} e^{-(k-\alpha)t} - \frac{\delta + \alpha}{2\alpha} e^{-(k+\alpha)t} \right). \quad (2)$$

$$[E.J] = [E.J]_\infty \left(1 - \frac{k + \alpha}{2\alpha} e^{-(k-\alpha)t} + \frac{k - \alpha}{2\alpha} e^{-(k+\alpha)t} \right). \quad (3)$$

$$v_0 = [E]_0 k_{s3} \frac{[S]_0}{[S]_0 + K_m}, \quad K_m = (k_{s2} + k_{s3})/k_{s1}. \quad (4)$$

$$v_s = \frac{v_0}{1 + (1 + 1/K_{43})[I]_0/K'_{21}}. \quad (5)$$

$$[E.I]_\infty = \frac{[E]_0}{1 + 1/K_{43} + K'_{21}/[I]_0}. \quad (6)$$

$$[E.J]_\infty = \frac{[E]_0}{1 + (1 + K'_{21}/[I]_0)K_{43}}. \quad (7)$$

$$K'_{21} = k_2/k'_1. \quad (8)$$

$$K_{43} = k_4/k_3. \quad (9)$$

$$k'_1 = k_1/(1 + [S]_0/K_m). \quad (10)$$

$$k = ([I]_0 k'_1 + k_2 + k_3 + k_4)/2. \quad (11)$$

$$\alpha = \sqrt{k^2 - k_2 k_4 - [I]_0 k'_1 (k_3 + k_4)}. \quad (12)$$

$$\beta = k - \frac{2k + k_3 + k_4 + (k_3 + k_4)^3/k_2 k_3}{1 + (k_3 + k_4)^2/k_2 k_3}. \quad (13)$$

$$\gamma = \frac{K'_{21}}{[I]_0} \cdot \frac{1/k_3 + (1 + K_{43})^2/k_2}{[1 + (1 + K'_{21}/[I]_0)K_{43}]^2}. \quad (14)$$

$$\delta = k - k_4 - k_3 + [I]_0 k'_1/K_{43}. \quad (15)$$

It is interesting to note several practically relevant properties of the above mathematical model for stepwise slow-binding inhibition. The reaction rate v_0 Eq. (4) is the uninhibited rate, i.e., the reaction rate that would be observed in the absence of inhibitor. The steady state rate v_s Eq. (5) is the asymptotic reaction rate that would be observed after all enzyme–inhibitor binding transients have subsided. The expression $v_0 \gamma$ in Eq. (1) represents a displacement on the

vertical (concentration) axis, where intersection occurs with the asymptotic straight line — the tangent to the reaction progress curve drawn at infinite reaction time.

The symbols $[E.I]_{\infty}$ Eq. (6) and $[E.J]_{\infty}$ Eq. (7) represent the concentrations of the corresponding enzyme–inhibitor complexes at equilibrium. The apparent bimolecular rate constant k'_1 Eq. (10) for enzyme–inhibitor association is smaller by a factor $1 + [S]_0/K_m$ relative to the true association rate constant, k_1 , because the inhibitor competes for binding with the substrate. The dissociation equilibrium constant $K'_{21} = k_2/k'_1$ is defined in terms of this apparent association rate constant k'_1 ; the true dissociation equilibrium constant of the initially formed enzyme–inhibitor complex, $E.I$, is $K_{21} = k_2/k_1$. The isomerization equilibrium constant $K_{43} = k_4/k_3$ characterizes the extent to which the initially formed enzyme–inhibitor complex would eventually rearrange, after equilibrium has been reached, into the final complex $E.J$.

The symbols k , α , β , $1/\gamma$, and δ formally are pseudo-first-order rate constants, variously dependent on the total concentrations of reactants and on the seven elementary rate constants appearing in the postulated reaction mechanism (Scheme 1).

Results

Several experimentally relevant applications of the newly derived theoretical model for slow-binding enzyme inhibition are here described.

Heuristic simulations of pre-steady state kinetics

The kinetic model represented by Eq. (1) through (3) can be used to visualize the pre-steady state progress of enzyme–inhibitor binding. For example, Fig. 1 shows the evolution of all enzyme species appearing in Scheme 1. The graph was generated by assuming purposely that the rate constants k_2 (for the dissociation of the initially formed enzyme–inhibitor complex) and k_3 (for the isomerization of the initially formed enzyme–inhibitor complex) are comparable in magnitude. This assumption could not have been made under currently published mathematical models for slow binding inhibition, which always assume that $k_2 \gg k_3$ (rapid equilibrium approximation).

From the graph in Fig. 1 we can gain valuable insight into the qualitative features of the steady state binding model. For example, let us consider the fact that the rate of product formation in Scheme 1 is proportional to the concentration of the enzyme–substrate complex, $[E.S]$. In Fig. 1, we can clearly see that the rate of product formation would gradually decrease throughout the entire pre-steady state phase, starting from $t = 1$ ms and continuing to $t = 100$ s. This is distinct from the conventional rapid-equilibrium approximation, according to which the rate of product formation decreases in two very distinct phases. In the first phase of the rapid-equilibrium treatment, the enzyme and inhibitor bind virtually instantaneously to form the complex $E.I$. Corresponding to

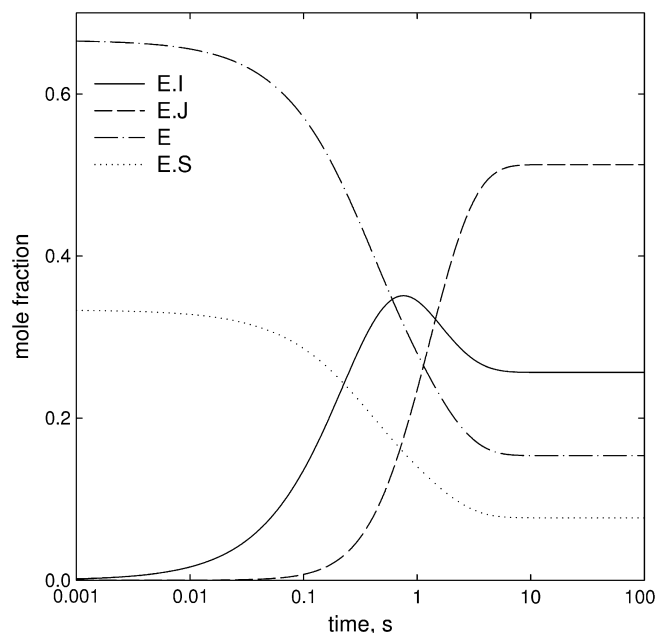


Fig. 1. Simulation of pre-steady state evolution of enzyme species in the reaction mechanism shown in Scheme 1, using Eqs. (2) and (3). The mole fractions of enzyme forms were simulated using the following values of model parameters: $k_{s1} = 1000 \mu\text{M}^{-1}\text{s}^{-1}$; $k_{s2} = 2000 \text{s}^{-1}$; $k_{s3} = 1 \text{s}^{-1}$; $k_1 = 2.0 \mu\text{M}^{-1}\text{s}^{-1}$; $k_2 = 1.5 \text{s}^{-1}$; $k_3 = 1.0 \text{s}^{-1}$; $k_4 = 0.5$, $[E]_0 = 0.001 \mu\text{M}$; $[S]_0 = 1 \mu\text{M}$; $[I]_0 = 1 \mu\text{M}$.

the extent of this instantaneous binding, we would observe a decrease in “initial velocity” with inhibitor concentration.

In contrast, Fig. 1 clearly shows that, under the more general steady state (as opposed to rapid-equilibrium) approximation, there is no distinct initial binding phase followed by subsequent isomerization of the initially formed enzyme–inhibitor complex. Therefore, the notion of initial velocity has a very different meaning in the formalism applied here, compared to that in the classical rapid-equilibrium theory. In fact, Fig. 1 illustrates that interpreting initial velocities in an actual experiment is bound to be exceedingly difficult if and when the rate constants k_2 and k_3 for a particular inhibitor are comparable in magnitude. As the Fig. 1 shows, the principal difficulty is that the reaction velocity changes continuously and smoothly, from very early on in the experiment (on the microsecond time scale).

Detecting deviations from the rapid-equilibrium model

Under the rapid-equilibrium approximation, it is assumed that the concentration reaction product P appearing in Scheme 1 increases according to Eq. (16) [1], where k_{obs} is the apparent first-order rate constant, V_s is the final steady state velocity, and V_0 is the initial reaction velocity.

$$[P] = \frac{V_0 - V_s}{k_{\text{obs}}} (1 - e^{-k_{\text{obs}}t}) + V_s t. \quad (16)$$

An important assumption underlying Eq. (16) is that the rate constant k_3 in Scheme 1 is negligibly small compared to k_2 . The question then arises; what if this simplifying

assumption (the rapid-equilibrium approximation) does not hold? Would clear systematic deviation between the experimental data and the presumed theoretical model be detectable under realistic experimental conditions?

To answer this question, Eq. (1) was used to generate artificial data, which were subsequently fit to Eq. (16). The results are shown in Fig. 2. The residual plot in the bottom panel of Fig. 2 is clearly nonrandom, which represents a systematic deviation between the presumed theoretical model (based on the rapid-equilibrium approximation) and the synthetic data (generated under the more general steady state approximation).

The results of this numerical experiment demonstrate that it is reasonable to expect an occasional failure of Eq. (16) as the mathematical model for slow binding inhibition data, even in the absence of inhibition depletion. If deviations are in fact found in the analysis of real-world experimental data and if the deviations are similar to those shown in Fig. 2, it may suggest that the inhibitor dissociation step ($E.I \rightarrow E + I$) is not very much faster than isomerization of the initial complex ($E.I \rightarrow E.J$).

Discrimination between one-step and two-step mechanisms

The determination of k_{obs} in Eq. (16) is an important component of a conventional method of discriminating

between the two-step mechanism in Scheme 1 and a single-step counterpart mechanism, in which the intermediate complex $E.I$ is absent. Specifically, it has been recommended to measure the dependence of k_{obs} on the inhibitor concentration $[I]_0$ and then determine whether the dependence is linear, which would suggest the single-step mechanism. In contrast, a nonlinear—more specifically, hyperbolic—dependence of k_{obs} on $[I]_0$ would suggest the involvement of the two-step mechanism. For review of this and other conventional methods of kinetic analysis used for slow-binding inhibitors, see [1].

We have shown above that the single-exponential model represented by Eq. (16) may not fit the experimental data if the rate constants k_2 and k_3 in Mechanism B are similar in magnitude. However, obvious systematic deviations similar to those shown in Fig. 2 may not always be detectable. The question then arises: does Eq. (16), in fact allow reliable discrimination between the one-step and the two-step models according to the conventional data-analytic protocol.

To answer this question, a family of progress curves using Eq. (1) as the theoretical model was generated. Following the usual experimental design, each progress curve was generated at a different total concentration of the inhibitor, $[I]_0$. The synthetic progress curves were then fit

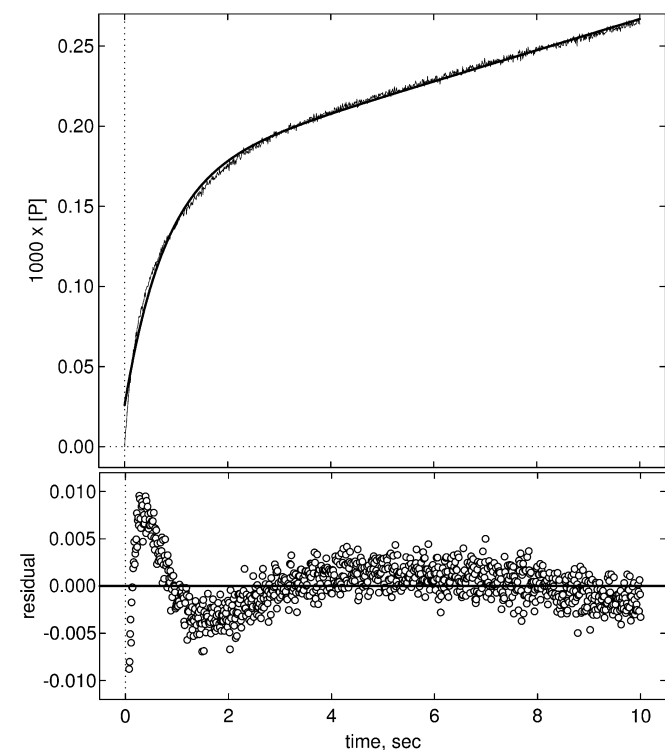


Fig. 2. Least-squares fit to Eq. (16) of artificial data simulated according to Eq. (1). The pseudoexperimental data were simulated using the following values of model parameters: $k_{s1} = 1000 \mu\text{M}^{-1}\text{s}^{-1}$; $k_{s2} = 1000 \text{s}^{-1}$; $k_{s3} = 1 \text{s}^{-1}$; $k_1 = 10 \mu\text{M}^{-1}\text{s}^{-1}$; $k_2 = 1 \text{s}^{-1}$; $k_3 = 1 \text{s}^{-1}$; $k_4 = 0.1$, $[E]_0 = 0.001 \mu\text{M}$; $[S]_0 = 1 \mu\text{M}$; $[I]_0 = 1 \mu\text{M}$.

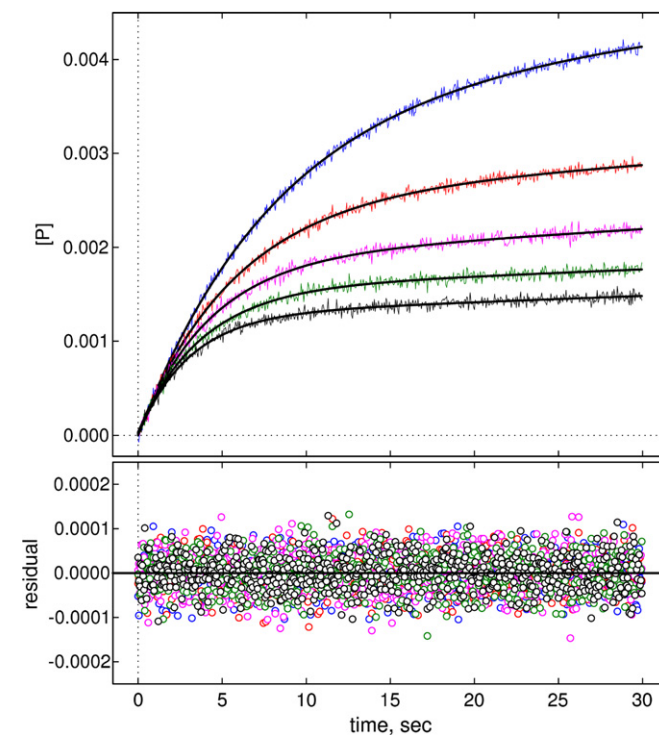


Fig. 3. Least-squares fit to Eq. (16) of artificial data simulated according to Eq. (1). The pseudoexperimental data were simulated using the following values of model parameters: $k_{s1} = 1000 \mu\text{M}^{-1}\text{s}^{-1}$; $k_{s2} = 1000 \text{s}^{-1}$; $k_{s3} = 1 \text{s}^{-1}$; $k_1 = 10 \mu\text{M}^{-1}\text{s}^{-1}$; $k_2 = 2 \text{s}^{-1}$; $k_3 = 2 \text{s}^{-1}$; $k_4 = 0.02$, $[E]_0 = 0.001 \mu\text{M}$; $[S]_0 = 1 \mu\text{M}$; $[I]_0 = 0.05 \mu\text{M}$ (blue), $0.075 \mu\text{M}$ (red), $0.1 \mu\text{M}$ (purple), $0.125 \mu\text{M}$ (green), $0.15 \mu\text{M}$ (black). The complete dataset additionally included two progress curves simulated at $[I]_0 = 0.175 \mu\text{M}$ and $0.2 \mu\text{M}$.

to Eq. (16), and a plot of k_{obs} against $[I]_0$ was constructed in an attempt to detect any deviations from linearity. Because this is a simulation experiment, we do know that the stepwise binding mechanism in Scheme 1 is the “true” model. Therefore, we do expect the plot of k_{obs} against $[I]_0$ to be nonlinear. The results are summarized in Figs. 3–5.

Fig. 3 shows that the traditional kinetic model, Eq. (16), does fit our simulated data exceedingly well. This is seen in the random distribution of residuals (bottom panel). However, contrary to expectation based on the traditional method of kinetic analysis, the plot of k_{obs} against $[I]_0$ appears linear (Fig. 4) even though the underlying true model is the two-step mechanism. From this we conclude that, under the more general steady state approximation used here, as opposed to the conventional rapid-equilibrium approximation, the concentration dependency of k_{obs} does not appear to be a reliable indicator of the enzyme–inhibitor binding mechanism.

Importantly, the best-fit values of the initial reaction rates (V_0 in Eq. (16)) do decrease with increasing total inhibitor concentration (Fig. 5). This is in agreement with the simulated (two-step) model. If the underlying mechanism included only a single enzyme–inhibitor binding step, the initial rate V_0 in Eq. (16) is not expected to vary with total inhibitor concentrations [1]. Thus, we conclude that the dependency of V_0 on $[I]_0$ appears to be a more reliable indicator of the binding mechanism (a single step vs two steps) compared to the dependency of k_{obs} on $[I]_0$, which is frequently used for model discrimination.

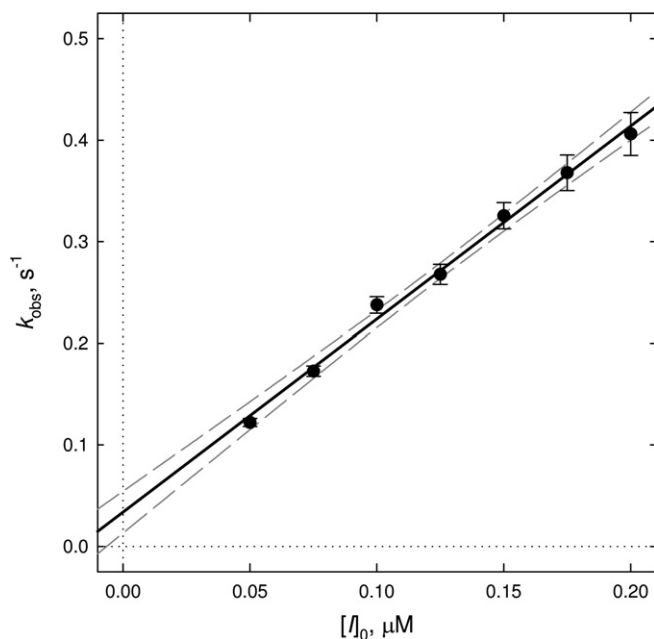


Fig. 4. Linear least-squares fit of apparent first-order rate constants, k_{obs} in Eq. (16), determined from simulated data shown in Fig. 3; see legend to Fig. 3 for values of simulated rate constants and concentrations. For a one-step mechanism, $E + I \rightleftharpoons EI$, the dependency is expected to be linear.

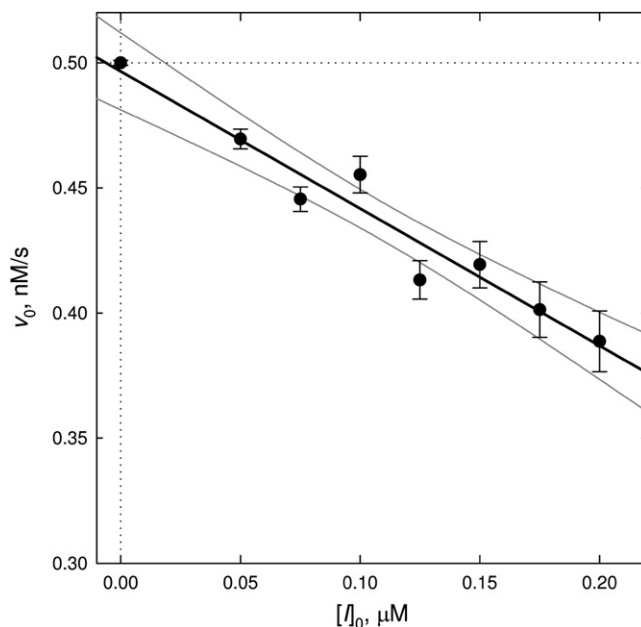


Fig. 5. Variation in the initial rates, V_0 in Eq. (16), determined from simulated data shown in Fig. 3; see legend to Fig. 3 for values of simulated rate constants and concentrations. For a one-step mechanism, $E + I \rightleftharpoons EI$, V_0 is not expected to change with $[I]_0$ (horizontal straight line).

Discussion

This paper was designed to answer the following question. Assuming that enzyme–inhibitor binding follows the two-step reaction mechanism shown in Scheme 1, and that there are specific numerical values for all rate constants that appear in this mechanism, what are the concentrations of reactants (the substrate and the product) and intermediates (enzyme species) at any given time? The question arises not only in heuristic simulations but also—more importantly—in the statistical analysis of real-world experimental data.

A fully general and most precise answer to the above question can be obtained only by numerical integration of a complete system of first-order ODEs, namely, Eqs. (17)–(23) shown in the Appendix. This numerical integration requires a sophisticated computer algorithm, an “ODE solver” which typically uses thousands of arithmetic operations merely to compute a single time point [5].

Although several specialized computer programs for this purpose have been available to practicing enzymologists [6,7], the requirement for a specialized software algorithm is a serious drawback in many circumstances. Therefore, we have set out to derive at least an approximate solution to the kinetic problem by adopting a series of simplifying assumptions. This allowed us to derive closed-form algebraic kinetic equations Eqs. (1)–(3). These equations can now be used to simulate or fit experimental data without relying on highly specialized ODE solver algorithms simply by encoding them in any standard spreadsheet, a generic data-fitting software program, or even a pocket calculator.

One such approximate solution has already been described in the literature, namely, Eq. (16) above, which is based on three simplifying assumptions about the enzyme system (for review, see [1]). First, Eq. (16) implies that both the inhibitor and the substrate are present in very large excess, relative to the total enzyme concentration, through the entire experiment (no inhibitor or substrate depletion). Second, Eq. (16) is based on the rapid-equilibrium approximation, implying that the dissociation of the initially formed enzyme–inhibitor complex ($E.I \rightarrow E + I$) is very much faster than the isomerization of this complex into its more tightly bound form ($E.I \rightarrow E.J$). In other words, the classic theoretical model assumes that the rate constant k_2 in Scheme 1 is very much larger than the rate constant k_3 .

In this work the assumption that the total concentrations of I and S are very high relative to the enzyme concentration was retained (otherwise no steady state algebraic solution could be derived in principle), but any restrictions on the relative values of kinetic constants appearing in the reaction mechanism were removed. Specifically, in contrast with the currently accepted mathematical models for slow-binding inhibition, we no longer require that the association and dissociation steps ($E + I \rightleftharpoons E.I$) are many orders of magnitude faster than the isomerization steps ($E.I \rightleftharpoons E.J$).

The removal of all restrictions on the relative values of rate constants produced an algebraic model for slow-binding inhibition that is more complex than the classic rapid-equilibrium rate equation. Specifically, instead of a single exponential term appearing in the traditional Eq. (16), we now have two distinct exponential terms appearing in Eq. (1). The appearance of the reaction product over time generally follows a double exponential plus a linear term.

Using heuristic simulations, our steady state kinetic model was used to investigate several aspects of slow-binding kinetics that have practical implications. For example, we found that, if the rate constants for dissociation and isomerization of $E.I$ are similar in magnitude, the appearance of product P over time in some cases — depending on complex relationships between all four rate constants appearing in the binding mechanism — shows detectable deviation from the traditional kinetic model, Eq. (16). The lesson learned is that if deviations similar to those in Fig. 2 were found in analyzing real-world experiments, it might suggest a relatively slow off-rate (a relatively low value of k_2) compared to isomerization (k_3). In such cases, Eq. (1) might be a better fitting model for the reaction progress than the traditional Eq. (16).

We also found that in certain other cases—again depending on complex relationships between the particular values of k_1 through k_4 —the deviations from the single exponential kinetic model Eq. (16) are not likely to be detected, even though the rapid-equilibrium approximation does not hold. This is illustrated in Fig. 3, simulated with $k_2 = k_3 = 2 \text{ s}^{-1}$. However, the main lesson learned from that particular simulation experiment is that the apparent

first-order rate constant k_{obs} in Eq. (16) is not a good indicator of the two-step vs one-step binding mechanism.

In particular, Fig. 4 shows that the dependence of k_{obs} on the total inhibitor concentration is essentially a straight line suggesting nominally the one-step mechanism, according to the classic kinetic analysis [1]. This result suggests that to properly discriminate between the various mechanistic models of slow binding enzyme inhibition, the simplified algebraic method of kinetic analysis might not be suitable. It is likely that a more fruitful approach to the slow-binding kinetics would be based on global analysis [8] of several enzyme progress curves combined together and treated as a single dataset, rather than (as is often done) fitting each progress curve separately and subsequently reanalyzing derived kinetic constants, such as k_{obs} or V_0 appearing in Eq. (16). An optimized data analytic protocol for slow-binding kinetic model discrimination is currently being investigated in this laboratory.

One important limitation of our approach is retaining the simplifying assumption that both substrate and inhibitor must be in very large excess over enzyme. This will limit the general utility of the algebraic model. As was correctly pointed out by a reviewer, the algebraic model described here is likely to be surpassed by the completely general approach based on numerically solving systems of differential equations as implemented for example in the software DYNAFIT [7]. However, an important advantage of the simplified algebraic approach (where applicable) is that it is computationally between one and two orders of magnitude faster. This allows us to perform important but very time-consuming numerical experiments, such as Monte Carlo simulations designed to study the intrinsic identifiability of kinetic constants appearing in the two-step slow-binding model.

In summary, we have presented a steady state mathematical model for slow-binding enzyme inhibition kinetics, assuming the validity of the two-step reaction mechanism in Scheme 1. The only assumption inherent in the model is that the total or analytic concentrations of substrate and inhibitor are very much higher than the concentration of the enzyme. Importantly, unlike mathematical models previously published in the literature, our model does not make any assumptions about the relative values of rate constants. Thus, the model allows a more general approach to heuristic simulations and to the statistical analysis of experimental data. Our kinetic model is implemented as a simple algebraic equation, which means that concentration changes over time can be computed using even hand calculators a simple spreadsheet program, or one of many conventional data analysis and visualization software packages.

Acknowledgment

The author is indebted to Sergei Gulnik (Sequoia Pharmaceuticals, Inc.) for stimulating discussions.

Appendix. Derivation of kinetic equations

The reaction mechanism in Scheme 1 is described by the complete set of differential equations

$$d[E]/dt = -k_{s1}[E][S] + k_{s2}[E.S] - k_1[E][I] + k_2[E.I], \quad (17)$$

$$d[S]/dt = -k_{s1}[E][S] + k_{s2}[E.S], \quad (18)$$

$$d[E.S]/dt = k_{s1}[E][S] - (k_{s2} + k_{s3})[E.S], \quad (19)$$

$$d[P]/dt = k_{s3}[E.S], \quad (20)$$

$$d[I]/dt = -k_1[E][I] + k_2[E.I], \quad (21)$$

$$d[E.I]/dt = k_1[E][I] - (k_2 + k_3)[E.I] + k_4[E.J], \quad \text{and} \quad (22)$$

$$d[E.J]/dt = k_3[E.I] - k_4[E.J]. \quad (23)$$

Assuming no substrate or inhibitor depletion ($[I] = [I]_0$, $[S] = [S]_0$), we can eliminate differential equations for $[I]$ and $[S]$:

$$d[E]/dt = -k_{s1}[E][S]_0 + k_{s2}[E.S] - k_1[E][I]_0 + k_2[E.I],$$

$$d[E.S]/dt = k_{s1}[E][S]_0 - (k_{s2} + k_{s3})[E.S],$$

$$d[P]/dt = k_{s3}[E.S],$$

$$d[E.I]/dt = k_1[E][I]_0 - (k_2 + k_3)[E.I] + k_4[E.J], \quad \text{and}$$

$$d[E.J]/dt = k_3[E.I] - k_4[E.J].$$

We now invoke the steady state approximation for the substrate portion of the mechanism. Thus,

$$K_m = (k_{s2} + k_{s3})/k_{s1},$$

$$\frac{[E.S]}{[E] + [E.S]} = \frac{[S]_0/K_m}{1 + [S]_0/K_m},$$

$$[E.S] = ([E] + [E.S]) \frac{1}{1 + K_m/[S]_0}, \quad \text{and}$$

$$[E] = ([E] + [E.S]) \frac{1}{1 + [S]_0/K_m}.$$

Utilizing the mass balance equation for the enzyme, we obtain for the steady state concentrations $[E]$ and $[E.S]$

$$[E]_0 = [E] + [E.S] + [E.I] + [E.J],$$

$$[E] + [E.S] = [E]_0 - [E.I] - [E.J],$$

$$[E.S] = ([E]_0 - [E.I] - [E.J]) \frac{1}{1 + K_m/[S]_0}, \quad \text{and}$$

$$[E] = ([E]_0 - [E.I] - [E.J]) \frac{1}{1 + [S]_0/K_m}.$$

This leads to the reduced system of three simultaneous differential equations for three unknowns:

$$d[P]/dt = ([E]_0 - [E.I] - [E.J]) \frac{k_{s3}}{1 + K_m/[S]_0},$$

$$d[E.I]/dt = ([E]_0 - [E.I] - [E.J]) \frac{k_1}{1 + [S]_0/K_m} [I]_0 - (k_2 + k_3)[E.I] + k_4[E.J], \quad \text{and}$$

$$d[E.J]/dt = k_3[E.I] - k_4[E.J].$$

For notational simplicity we can define the apparent first-order rate constants k_0 and k'_1 as

$$k_0 \equiv \frac{k_{s3}}{1 + K_m/[S]_0} \quad \text{and}$$

$$k'_1 \equiv \frac{k_1}{1 + [S]_0/K_m}.$$

The final system of differential equations to be solved is

$$d[P]/dt = k_0([E]_0 - [E.I] - [E.J]),$$

$$d[E.I]/dt = k'_1[I]_0[E]_0 - (k'_1[I]_0 + k_2 + k_3)[E.I] + (k_4 - k'_1[I]_0)[E.J], \quad \text{and}$$

$$d[E.J]/dt = k_3[E.I] - k_4[E.J].$$

Setting the initial conditions $[P]_{t=0} = [E.I]_{t=0} = [E.J]_{t=0} = 0$, we can now apply the method of Laplace transforms to obtain the integral equation for the concentration of the reaction product $[P]$ and the concentrations of the enzyme-inhibitor complexes:

$$[P] = v_0 \gamma \left(1 + \frac{\beta}{\alpha} e^{-kt} \sinh(\alpha t) - e^{-kt} \cosh(\alpha t) \right) + v_s t,$$

$$[E.I] = [E.I]_{\infty} \left(1 + \frac{\delta}{\alpha} e^{-kt} \sinh(\alpha t) - e^{-kt} \cosh(\alpha t) \right), \quad \text{and}$$

$$[E.J] = [E.J]_{\infty} \left(1 - \frac{k}{\alpha} e^{-kt} \sinh(\alpha t) - e^{-kt} \cosh(\alpha t) \right).$$

All auxiliary variables (α , β , k , etc.) are defined in the text under Theory.

The hyperbolic sine and cosine functions in the expressions above are not useful for practical computations, because even a relatively small numeric argument for $\sinh(x)$ and $\cosh(x)$ leads to numerical overflow. We found this to be true even for relatively small reaction times. Therefore, the integral equations above were algebraically rearranged by taking into account the definitions $\sinh x = (e^x - e^{-x})/2$ and $\cosh x = (e^x + e^{-x})/2$. Grouping all exponential terms, we obtained the final kinetic equations (1)–(3). A similar derivation has been presented by Sculley et al. [9].

SigmaPlot simulation script

The following code represents a simulation “transform,” or script, which was used to compute the changes in product concentration over time in the commercial data analysis software package SigmaPlot (Systat Software Inc., San Jose, California). Similar code can be created for many other commercial software packages commonly used for biochemical data analysis.

```

;-----
; Generate 100 time points from zero to 10
seconds:
t = data(0,10,0.1)
; Rate constants appearing in the two-step
mechanism
; Units: uM, sec
ks1 = 1000
ks2 = 2000

```

```

ks3 = 1
k1 = 10
k2 = 1
k3 = 1
k4 = 0.1
; Total concentrations
; Units: uM
Eo = 0.001
So = 1
Io = 1
; The model (product concentration over
time):
Km = (ks2+ks3)/ks1
klp = k1/(1+So/Km)
K21 = k2/klp
K43 = k4/k3
v0 = Eo*ks3*(So/Km)/(1+So/Km)
vs = v0/(1+(1+1/K43)*(Io/K21))
k = (Io*klp+k2+k3+k4)/2
alpha = sqrt(k*k-Io*klp*(k3+k4)-k2*k4)
beta = k-(2*k+k3+k4+(k4+k3)^3/(k2*k3))/
(1+(k4+k3)^2/(k2*k3))
gamma = (K21/Io)*(1/k3+(1+K43)^2/k2)/
(1+(1+K21/Io)*K43)^2
exp1 = exp(-(k-alpha)*t)*(beta-alpha)/
(2*alpha)
exp2 = -exp(-(k+alpha)*t)*(beta+alpha)/
(2*alpha)
P = v0*gamma*(1+exp1+exp2)+vs*t

```

```

; Put the simulated data (time vs. concen-
tration) in the first
; two columns in the SigmaPlot spreadsheet
file:
put t into col(1)
put P into col(2)
;-----

```

References

- [1] S. Szedlacsek, R.G. Duggleby, Kinetics of slow and tight-binding inhibitors, *Meth. Enzymol.* 249 (1995) 144–180.
- [2] S. Cha, Tight binding inhibitors. I. kinetic behavior, *Biochem. Pharmacol.* 24 (1979) 2177–2185.
- [3] J.W. Williams, J.F. Morrison, The kinetics of reversible tight-binding inhibition, *Meth. Enzymol.* 63 (1979) 437–467.
- [4] E. Kreyszig, *Advanced Engineering Mathematics*, 7th ed., John Wiley, New York, 1993.
- [5] G.D. Byrne, A.C. Hindmarsh, Stiff ODE solvers: a review of current and coming attractions, *J. Comput. Physics* 70 (1987) 1–62.
- [6] B.A. Barshop, R.F. Wrenn, C. Frieden, Analysis of numerical methods for computer simulation of kinetic processes: development of KINSIM—a flexible, portable system, *Anal. Biochem.* 130 (1983) 134145.
- [7] P. Kuzmič, Program DYNAFIT for the analysis of enzyme kinetic data: Application to HIV proteinase, *Anal. Biochem.* 237 (1996) 260–273.
- [8] J.M. Beechem, Global analysis of biochemical and biophysical data, *Meth. Enzymol.* 210 (1992) 37–54.
- [9] M.J. Sculley, J.F. Morrison, W.W. Cleland, Slow binding inhibition: the general case, *Biochim. Biophys. Acta* 1298 (1996) 78–86.